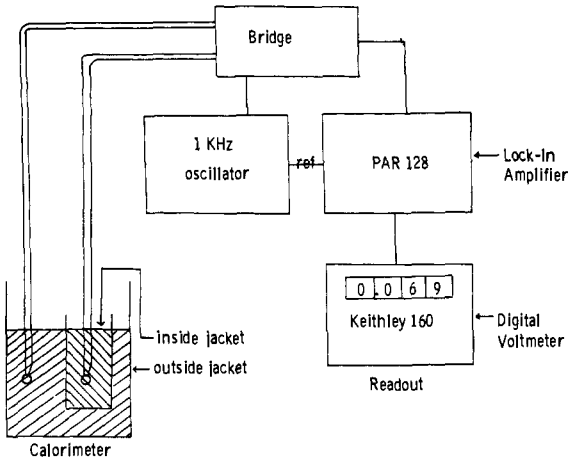


**Figure 7.** Schematic diagram for the calorimeter used.

the thermistors. A block diagram of the apparatus used can be seen in Figure 7.

A 1 kHz oscillator powers a modified Wheatstone bridge and at the same time provides the reference signal for the null detector. In our case, the null detector is a Princeton Applied Research 128 Lock-in Amplifier. The basic innovation on the ac bridge is the use of operational amplifiers to provide gain and low noise of the unbalanced ac signal. The null detector output (−1.0 to 1.0 V) was connected to a Keithley 160 digital voltmeter, where the unbalanced signal was monitored. When the thermistors were placed inside their respective jackets of the calorimeter, the variable resistors of the ac bridge were changed until the lock-in detector read a null. From this point on, the voltage detected by the lock-in amplifier was interpreted as a temperature difference between the two probes. Calibration showed that the unbalanced signal is a linear function of the temperature difference of the two probes with a slope of 1.80 ± 0.01 μV/mdeg, at temperatures where these experiments were carried out. This technique can provide a thermal resolution of 1 μdeg and an accuracy of 0.1% in the millidegree region.

The Toepler Pump connected with the gas buret and NMR systems have been previously described.[17]

**Acknowledgment.** The authors are grateful to Research Corporation, The National Institute of Health, and the donors of the Petroleum Research Fund, administered by the American Chemical Society, for support of this work. The NIH support was from Grant No. RR-8102 from the division of Research Resources.

## References and Notes

(1) H. L. Strauss, T. J. Katz, and G. K. Fraenkel, *J. Am. Chem. Soc.*, **85**, 2360 (1963).
(2) J. F. M. Oth and G. Schröder, *J. Chem. Soc. B*, 904 (1971).
(3) J. F. M. Oth, H. Baumann, J. M. Gilles, and G. Schröder, *J. Am. Chem. Soc.*, **94**, 3498 (1972).
(4) E. J. Prosen, "Experimental Thermochemistry", Vol. 1, F. D. Rossini, Ed., Wiley-Interscience, New York, N.Y., 1956, p 129.
(5) (a) W. D. Good, D. W. Scott, and G. Waddington, *J. Phys. Chem.*, **60**, 1080 (1956); (b) C. A. Neugebauer and J. L. Margrave, *ibid.*, **62**, 1043 (1958).
(6) D. R. Thielen and L. B. Anderson, *J. Am. Chem. Soc.*, **94**, 2521 (1972).
(7) R. B. Turner, W. R. Meador, W. von E. Doering, L. H. Knox, J. R. Mayor, and D. W. Wiley, *J. Am. Chem. Soc.*, **79**, 4127 (1957).
(8) G. R. Stevenson and I. Ocasio, *J. Phys. Chem.*, **79**, 1387 (1975).
(9) S. Z. Goldberg, K. N. Raymond, C. A. Harman, and D. H. Templeton, *J. Am. Chem. Soc.*, **96**, 1348 (1974).
(10) E. E. Ketchen and W. E. Wallace, *J. Am. Chem. Soc.*, **73**, 5810 (1951).
(11) F. D. Rossini, D. D. Wagman, W. H. Evans, S. Levine, and I. Jaffe, *Natl. Bur. Stand. (U.S.) Circ.*, 9, 819 (1952).
(12) F. A. L. Anet, *J. Am. Chem. Soc.*, **84**, 671 (1962).
(13) G. R. Stevenson, *J. Chem. Educ.*, **49**, 781 (1972).
(14) G. R. Stevenson and I. Ocasio, *J. Am. Chem. Soc.*, **98**, 890 (1976).
(15) (a) G. R. Hedwig, D. A. Owensby, and A. J. Parker, *J. Am. Chem. Soc.*, **97**, 3888 (1975); (b) B. G. Cox and A. J. Parker, *ibid.*, **95**, 402 (1973).
(16) G. R. Stevenson and J. G. Concepcion, *J. Phys. Chem.*, **76**, 2176 (1972).
(17) G. R. Stevenson and L. Echegoyen, *J. Am. Chem. Soc.*, **96**, 3381 (1974).
(18) J. I. Brauman and L. K. Blair, *J. Am. Chem. Soc.*, **90**, 6561 (1968).
(19) M. J. S. Dewar, A. Harget, and E. Haselbach, *J. Am. Chem. Soc.*, **91**, 7521 (1969).
(20) W. E. Wentworth and W. Ristau, *J. Phys. Chem.*, **73**, 2126 (1969).

# The Dioxygen Adduct of *meso*-Tetraphenylporphyrinmanganese(II), a Synthetic Oxygen Carrier

**Brian M. Hoffman,*[1] Charles J. Weschler, and Fred Basolo*[1]**

*Contribution from the Department of Chemistry, Northwestern University, Evanston, Illinois 60201.* *Received February 13, 1976*

**Abstract:** In toluene solutions (−79 °C) dioxygen reversibly binds to Mn(TPP)(py) with replacement of the pyridine to form a five-coordinate complex, rather than by addition to yield a six-coordinate species. The resulting Mn(TPP)($O_2$) complex surprisingly exhibits the $S = 3/2$ spin state ($D = -2.48 \pm 0.07$ cm$^{-1}$; $\lambda = E/D = 0.3257 \pm 0.0003$; $A_z = -53.1\ (\pm 0.5) \times 10^{-4}$ cm$^{-1}$; $A_y = -82.0\ (\pm 0.5) \times 10^{-4}$ cm$^{-1}$; $A_{17O} \doteq B_{17O} \doteq 0$). The experimental results, in combination with qualitative bonding considerations, indicate (i) extensive Mn → $O_2$ charge transfer and (ii) the appropriateness of an $Mn^{IV}(O_2^{2-})$ valency formalism in which the Mn(IV) is in the $^4(t_2^3)$ ground state. A linear geometry for the complex can be ruled out. Although further definite conclusions as to structure are not presently possible, we tentatively favor the symmetric, "edge-on" mode of binding.

Studies of dioxygen binding to transition metal complexes are of intrinsic importance, and in addition provide opportunities to attack the fundamental problems of the biological oxygen carriers and oxygenases. The properties of synthetic cobalt(II) and, more recently, iron(II) oxygen carriers have been intensively studied,[2] but manganese(II) was not found to reversibly bind dioxygen.[3]

One way to obtain oxygen adducts of synthetic iron(II) complexes is to use aprotic solvents and low temperatures.[4] Under such conditions the rate of irreversible formation of the stable μ-oxo dimer $Fe^{III}$-O-$Fe^{III}$ is negligibly slow, and the dioxygen binding is reversible. Since at ambient temperatures a pyridine (py) solution of manganese(II) phthalocyanine (Pc) is oxidized in air to yield (py)(Pc)$Mn^{III}$-O-$Mn^{III}$(Pc)(py),[5]

we decided to study the interaction between $O_2$ and a manganese(II) porphyrin at low temperatures in order to avoid the formation of a $\mu$-oxo dimer. Because the ease of oxidation (M(II) → M(III)) of a manganese(II) porphyrin is greater than that for a corresponding iron(II) complex,[6] it was expected that if irreversible side-reactions could be suppressed, then a manganese(II) system would bind dioxygen more tightly.

The above approach is successful, and our initial report[7] of the interaction between *meso*-tetraphenylporphyrin(pyridine)manganese(II), Mn(TPP)(py), and dioxygen indicated that a reversible dioxygen adduct is formed; this adduct was observed independently by Reed and co-workers.[8] However, its properties differ dramatically from those of cobalt and iron adducts:[2,4] oxygen binds to manganese with replacement of the pyridine ligand to form a five-coordinate complex (counting dioxygen as a single ligand) rather than by addition to yield a six-coordinate species, and the resulting Mn(TPP)($O_2$) complex surprisingly exhibits the $S = 3/2$ spin state.[7] We now present a complete optical and EPR study of this unusual compound.

## Experimental Section

**Materials.** The $^{17}O$ isotopically enriched $O_2$ was obtained from Miles (Elkhart, Ind.). Anal. 54.101% $^{17}O$, 0.704% $^{18}O$. Matheson prepurified nitrogen was passed through two chromous scrubbers and subsequently dried by sulfuric acid followed by KOH/Drierite. Matheson extra dry oxygen was further dried for optical work by bubbling through toluene at −79°. Toluene (Mallinckrodt "Analytical Reagent") was distilled from $LiAlH_4$ and stored over Na wire. All other chemicals were of reagent grade. *meso*-Tetraphenylporphyrin(pyridine)manganese(II), Mn(TPP)(py), was prepared by the method of Kobayashi and Yanagawa.[9] Anal. Calcd for [Mn($C_{44}H_{28}N_4$)($C_6H_5N$)]: C, 78.18; H, 5.22; N, 9.30. Found: C, 77.42; H, 4.54; N, 9.06.

**Analyses.** Elemental analyses of C, H, and N were performed by H. Beck of this department.

**Equipment.** Visible and ultraviolet spectra were recorded on a Cary Model 14 spectrophotometer. The low temperature optical studies were performed using a Pyrex cell (W. Sales Ltd., Deerfield, Ill.) mounted in a Dewar.[10] EPR spectra were taken on a Varian Associates E-4 EPR spectrometer, equipped with a Hewlett-Packard X-532-B frequency meter. Absolute field calibrations were checked with DPPH powder ($g = 2.0036$) and with a frozen solution of hemin fluoride ($g_\perp = 6.00$, $g_\parallel = 2.00$). Cooling was provided either by liquid nitrogen or liquid helium in Dewars of standard design.

**General Procedures.** For the preparation of air-sensitive solutions for optical work, the manganese complex was added to the cold temperature cell. It was then flushed with $N_2$ for at least 2 h, before cooling to about −45°. Using a gas-tight syringe, 20 ml of nitrogen saturated solvent was slowly dripped down the sides of the cooled cell, and nitrogen was bubbled through the mixture for about 0.5 h to effect dissolution. The cell was then cooled to −79° and the visible spectrum recorded to confirm the presence of a manganese(II) species.

Oxygen adducts were formed by bubbling prechilled oxygen through cold solutions of the manganese(II) complex. The presence of the adduct was confirmed by its visible spectrum. To determine reversibility of adduct formation, $N_2$ was bubbled through the solution until there was no further change in the visible spectrum. Such a procedure largely returns the spectrum to that initially observed.

The preparation of air sensitive solutions for EPR measurements was conducted on a vacuum line. Solid Mn(TPP)(py) was placed in an EPR tube provided with a vacuum O-ring joint and a Kontes Teflon vacuum valve. Dry, degassed toluene was then trap-distilled into the tube. After complete dissolution, the samples were frozen in liquid nitrogen and the EPR spectra recorded.

These samples would be oxygenated by exposure to oxygen at −79°. In a typical experiment employing $^{17}O$ enriched $O_2$, the EPR tube containing Mn(TPP)(py) in toluene was evacuated at liquid nitrogen temperature. Using gas-tight syringe and serum cap techniques, 5 $cm^3$ of $^{17}O$ enriched $O_2$ (at room temperature and pressure) was added to the EPR tube. Within 5 min of oxygenation, the samples were refrozen in liquid nitrogen and the EPR spectra recorded. Reevacuation was accomplished by freeze–pump–thaw cycles, taking care not to raise the temperature of the toluene solution above −79°.

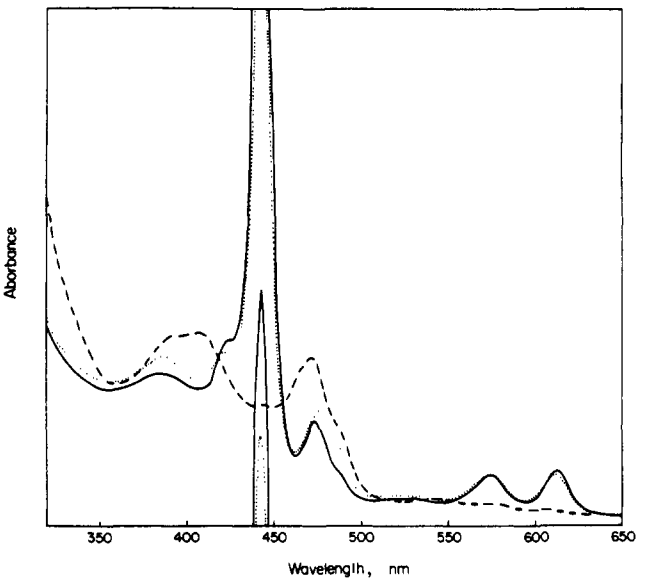


Figure 1. Optical spectrum of ~1 × $10^{-6}$ F Mn(TPP)(py) in toluene at −79°: (—) under nitrogen, (- - -) under oxygen, (· · ·) under nitrogen after oxygenation–deoxygenation cycle.

**Computations.** Computer calculations of EPR absorption fields were performed on a CDC 6400 using a modification of program EPR, written by Gladney and available from the Quantum Chemistry Program Exchange (no. 134), appropriately corrected to handle hyperfine terms in the presence of large zero-field splittings.

## Results

**I. Optical Spectroscopy.** A toluene solution (−79 °C) of Mn(TPP)(py) exhibits a typical metalloporphyrin optical spectrum (Figure 1), with an intense Soret peak and weaker $\alpha$ and $\beta$ peaks; wavelengths and extinction coefficients are in Table I. The sample is partially oxidized, as evidenced by additional absorptions at the positions of the "split Soret" peaks of the $Mn^{III}$(TPP) pyridine adduct (~475 and 380 nm). A more expanded presentation of the 500–700 nm region (Figure 2A) shows the $\alpha$ band to be slightly more intense than $\beta$, and also an additional weaker feature at 533 nm. No other peaks are observed at wavelengths shorter than 850 nm.

Upon exposure of the complex to oxygen (1 atm) at −79°, the spectrum changes to that shown in Figures 1 and 2B. The optical density decreases markedly and the Soret band splits, with the long-wavelength half appearing at 472 nm; these changes are similar to those observed upon going from $Mn^{II}$(TPP) to an $Mn^{III}$(TPP) species (Table I). New, weaker bands appear in the $\alpha$–$\beta$ region at 638 and 542 nm (Figure 2A); these positions are not identical with those of the $Mn^{III}$(TPP) in pyridine (617 and 588 nm). In addition, a substantially weaker peak appears at 820 nm ($\epsilon$ 1 × $10^3$ $M^{-1}$ $cm^{-1}$). All $Mn^{III}$(TPP)(X) complexes similarly show near-ir transitions;[11] the two longest wavelength peaks for pyridine solutions are of roughly equal intensity and fall at 833 and 781 nm.

The effect of oxygenation occurs within the time required to record the visible spectrum (several minutes after the addition of $O_2$). Removal of dioxygen (effected by bubbling rigorously dried and deoxygenated $N_2$ through the solution) largely returns the spectrum to that initially observed (Figures 1, 2C), and it is possible to go through several such oxygenation–deoxygenation cycles. Thus, Mn(TPP)(py) reacts reversibly with $O_2$ in toluene at −79°. Under these conditions, after 14 h of exposure to 1 atm $O_2$, 70% of the initial manganous complex can be regenerated. In contrast oxygenation of

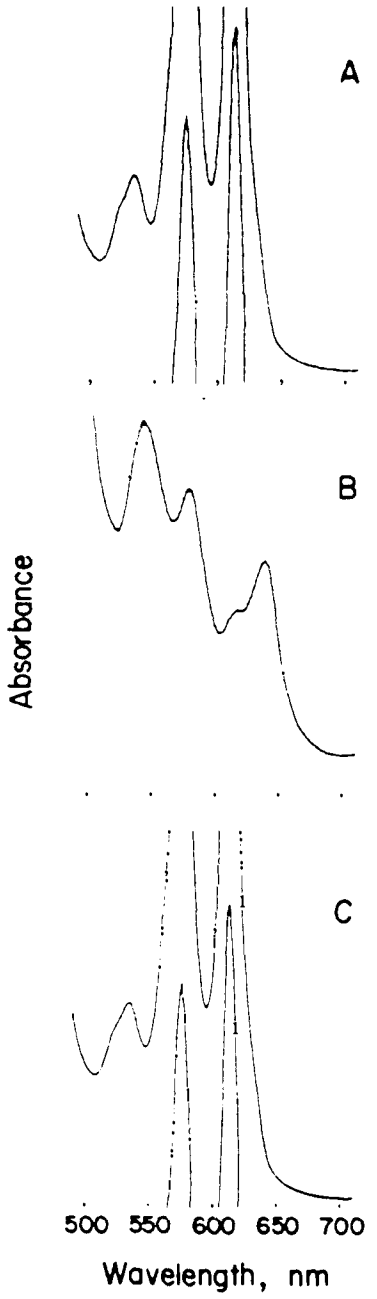


Figure 2. Visible spectrum of ~2 × $10^{-4}$ F Mn(TPP)(py) in toluene at −79°: (A) under nitrogen; (B) under 1 atm $O_2$; (C) under nitrogen after oxygenation–deoxygenation cycle.

Mn(TPP)(py) in toluene at room temperature or even at −45° rapidly leads to irreversible oxidation.

It was not feasible to determine reaction stoichiometry by gas uptake techniques as accomplished earlier for the analogous Fe(TPP)(py)$_2$.[12] At −79° the attainable concentration of Mn(TPP)(py) in toluene was insufficient to produce changes detectable on a 2-cm$^3$ gas buret (monitoring volume of $O_2$ at constant temperature and pressure). At higher temperatures where the toluene solubility of Mn(TPP)(py) was significantly greater (e.g., −45°), the manganous porphyrin oxidized irreversibly upon exposure to oxygen. There is the additional complication that in toluene at −79°, 1 atm of $O_2$, the oxygen adduct is not fully formed (determination of $K_{eq}$ is presently in progress; an initial estimate gives $K_{eq} \sim 0.1$). In solvents such as methylene chloride, which are expected to favor formation of the oxygen adduct,[10] a significant amount of irreversible oxidation occurs even at −79°.

Table I. Absorption Spectra

| $Mn^{II}$(TPP)(py) | | Mn(TPP)($O_2$) | |
|---|---|---|---|
| $\lambda_{max}$, nm | $\epsilon$, $M^{-1}$ cm$^{-1}$[a] | $\lambda_{max}$, nm | $\epsilon$, $M^{-1}$ cm$^{-1}$[a] |
| 612 | 1.3 × $10^4$ | 820 (833, 781)[b] | 0.12 × $10^4$ |
| 574 | 1.2 × $10^4$ | 638 (617) | 0.4 × $10^4$ |
| 533 | 0.37 × $10^4$ | 542 (580) | 0.7 × $10^4$ |
| 442 | 69. × $10^4$ | 472 (475) | 16.0 × $10^4$ |
| | | ~400 (380) | |

[a] Relative extinction coefficients are measured directly at −79° with reference to the 442-nm band of Mn(TPP)(py). Absolute values are only approximate, since they assume the room temperature value of $\epsilon$ for this reference band.[9] [b] Values in parentheses are the $\lambda_{max}$ for $Mn^{III}$(TPP)(py) from ref 11.

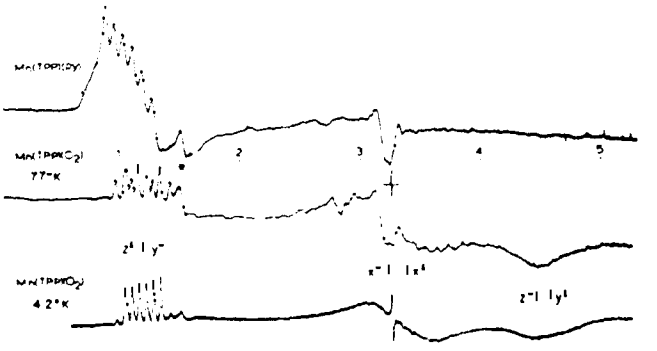


Figure 3. EPR spectrum of (A) (upper) Mn(TPP)(py) in degassed toluene at 77 K; (B) (middle) Mn(TPP)($O_2$) in toluene at 77 K; (C) (lower) Mn(TPP)($O_2$) in toluene at 4.2 K. Field calibration indicated in kG. Asterisk "*" indicates signal from rhombic iron in quartz. Resonance positions for Mn(TPP)($O_2$) calculated from the parameters in Table I for the external field along the magnetic $x,y,z$ axes are also shown; u and l refer to transitions within upper and lower Kramers doublets, respectively.

**II. EPR Spectroscopy. EPR of Mn(TPP)(py).** The 77 K EPR spectrum of a toluene solution of Mn(TPP)(py) is shown in Figure 3A. No change is observed when the spectrum is taken at 4.2 K. The shape of the low-field six-line $^{55}$Mn hyperfine pattern (splitting, 74 G) indicates an axial $g$-tensor with $g_\perp^{Mn} = 5.96$. Better spectra of the complex are obtainable, and they further show the features associated with the unique $g$ value at $g_\parallel = 2.00$. The $^{55}$Mn hyperfine interaction is essentially isotropic with $a^{Mn} = 74$ G $\simeq 69.1 \times 10^{-4}$ cm$^{-1}$.

The observed axial $g$ values are typical of a high-spin ($S = 5/2$) $d^5$ system with tetragonal zero-field splitting parameter ($D$) greater than the microwave quantum ($\tilde{\nu} \sim 0.3$ cm$^{-1}$). Experiments at Q-band ($\tilde{\nu} \sim 1.2$ cm$^{-1}$) show that for Mn(TPP)(py), $D^{Mn} \sim 0.55$ cm$^{-1}$.[13a] The large $D$ value for a Mn(II) ion, the lack of variation of the spectrum with base concentration, and the similarity to spectra of Mn-substituted hemoglobin[14] all led us to conclude that this spectrum is associated with the *five-coordinate* Mn(TPP)(py): this has been confirmed by an x-ray crystal structure.[8] Modest variations in $D$ are observed upon variation[13a] or removal[13b] of the neutral axial ligand.

**EPR of Mn(TPP)($O_2$).** In the presence of $O_2$ and excess pyridine (10–100% v/v) the Mn(TPP)(py) complex is stable at room temperature for as long as several hours, and the 77 K EPR spectrum (Figure 3A) is not affected by $O_2$. However, when Mn(TPP)(py) is dissolved in toluene, exposed to $O_2$ at −79°, and frozen, the 77 K spectrum of Figure 3B appears, with features at $g_3 = 1.45$, $g_2 \sim 2$, and $g_1 \sim 5.4$–$5.5$ (see Figure 4 and discussion below). In some samples an additional weak complicated spectrum with $g \simeq 2$, associated with an uncharacterized dimeric species, overlaps the broad $g \sim 2$ absorption (Figure 3B, but not 3C). Reevacuation restores the Mn(TPP)(py) spectrum, typically with a slight irreversible

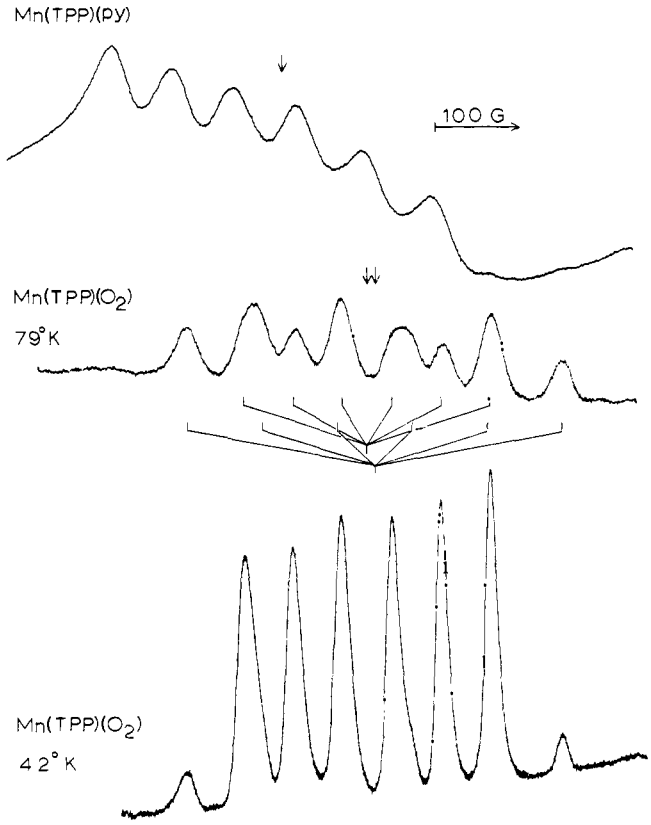


Figure 4. Low field portion of EPR spectrum of (A) (upper) Mn(TPP)(py) in degassed toluene; (B) (middle) Mn(TPP)($O_2$) in toluene at 77 K; and (C) (lower) Mn(TPP)($O_2$) in toluene at 4.2 K. The position of $g_\perp$ for Mn(TPP)(py) and the overlapping sextets in the Mn(TPP)($O_2$) spectrum are indicated.

increase of the multiline $g \simeq 2$ spectrum. This cycling can be repeated, indicating that the spectrum in Figure 3B is that of the reversible dioxygen adduct.

The overall shape of the dioxygen adduct spectrum is that of Kramers doublet with rhombic $g$ tensor. However, the low field portion of the spectrum (Figure 4) is found to consist of an overlapping of one sextet of equal intensity lines having ($g_1^l = 5.470$, $A^l = 57$ G), with another sextet having ($g_1^u = 5.424$, $A^u = 88$ G). Thus, the spectrum is a superposition from two Kramers doublets with slight differences in at least $g_1$. The two doublets, however, belong to the same chemical entity and are in thermal equilibrium. Changing the temperature of the frozen solution from 77 to 4.2 K reversibly changes the spectrum from that of Figure 3B and 4B where both doublets have equal EPR intensities ($I$) to that of Figure 3C and 4C where the enhanced spectrum from the (l) doublet shows it to be the one which is lower in energy. At 4.2 K the ratio of intensities of upper (u) to lower doublet is $I^u/I^l = 0.14$, which corresponds to an energy separation between them of $\Delta = 5.82 \pm 0.07$ cm$^{-1}$.

The unequal intensities of u and l doublets at 4.2 K permit the overlapping $^{55}$Mn hyperfine sextets to be even more clearly resolved than at 77 K (Figure 3C, 4C). In addition, the high field edge of the feature associated with the smallest $g$ value, $g_3$, is apparently accentuated at 4.2 K as compared to that at 77 K (Figure 3), indicating that $g_3$ for the two doublets differ, with $g_3^l < g_3^u$.

This observation of sextets, rather than an 11-line pattern with unequal intensity, indicates that the species formed is a 1:1 complex of manganese TPP and dioxygen. The above noted competition between pyridine and dioxygen further shows that the reaction is *not* $O_2$ addition to five-coordinate Mn. Rather, the observed reaction is a ligand replacement, and the low value

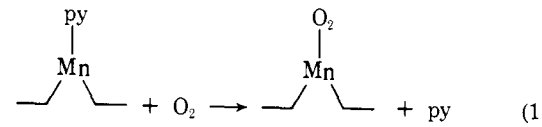


(1)

of $K_{eq}$ indicates that the affinity for $O_2$ is actually less than that for the nitrogenous ligand. This conclusion explains why manganese(II) hemoglobin does not bind $O_2$ reversibly.[3] The protein provides an adjacent imidazole as ligand to the Mn(II) porphyrin. With this high effective local concentration of coordinating base, the equilibrium (1) is driven to the left.

Experiments were also performed using 50% $^{17}$O enriched $O_2$. The experiment was repeated several times, and *no* effect of the isotopic substitution could be detected. No new peaks were observed even though the low-field region was scanned with particular care. Neither did the line widths of the resolved $^{55}$Mn hyperfine lines measurably change. We conclude that the *spin* density on the dioxygen moiety of Mn(TPP)($O_2$) is effectively zero.

**Analysis of Mn(TPP)($O_2$) EPR Spectra.** There are numerous electronic structures which may be conceived for this dioxygen adduct. The Mn(TPP)($O_2$) spectra of Figures 3 and 4 are wholly different from those observed for $O_2^-$ and for cobalt dioxygen adducts which are formulated[2] as Co(III)-$O_2^-$. This fact plus the large $^{55}$Mn hyperfine splittings and the absence of spin transfer to dioxygen found in the experiments with 50% $^{17}$O enriched $O_2$ rule out a similar electronic structure for the dioxygen complexes of the two metals, and thus a formulation as low-spin Mn(III)-$O_2^-$. In addition, the trio of $g$ values calculated from the observed peak positions can be shown by Blumberg's technique[15] to be inconsistent with any combination of crystal field parameters describing a low spin ($S = \frac{1}{2}$) $d^5$ Mn(II) ion. Finally, the overall shape plus other considerations ruled out an interpretation in terms of a high-spin ($S = \frac{5}{2}$), Mn$^{II}$(TPP)($^1O_2$).

With the above formulations excluded, and noting the similarity of the present spectra to those of certain ($d^3$) $S = \frac{3}{2}$ Cr(III) systems (neglecting hyperfine splitting),[16] we were led to consider the adduct as an $S = \frac{3}{2}$ system with large axial splitting, $D \gg 0.3$ cm$^{-1}$, and also a large rhombic distortion, $E$, with $E/D > 0.3$.[7] We now present the details of the analysis, and show it to totally accommodate the EPR spectra of Mn(TPP)($O_2$).

For an $S = \frac{3}{2}$ system, the spin Hamiltonian takes the form[17]

$$\mathcal{H} = \beta_e[g_xH_xS_x + g_yH_yS_y + g_zH_zS_z] + D[(S_z^2 - \tfrac{5}{4}) + \lambda(S_x^2 - S_y^2)] + [A_xS_xI_x + A_yS_yI_y + A_zS_zI_z]$$

where $\lambda = E/D$ is the ratio of rhombic to tetragonal crystal field parameters and $g_i$ and $A_i$ are the $g$ and hyperfine tensor principal axis components. The physically meaningful range of $\lambda$ is $0 \leq \lambda \leq \frac{1}{3}$, with $\lambda = 0$ corresponding to axial and $\lambda = \frac{1}{3}$ to purely rhombic symmetries. In general the $g$ tensor is nearly isotropic, $g_x \doteq g_y \doteq g_z = g$, with $g \lesssim g_e$ for an $S = \frac{3}{2}$ ion (e.g., $Cr^{3+}$, $Mn^{4+}$). In the absence of a magnetic field, and neglecting hyperfine couplings, the four states of the $S = \frac{3}{2}$ manifold split into two Kramers doublets which are separated in energy by

$$\Delta = 2(D^2 + 3E^2)^{1/2} = 2|D|(1 + 3\lambda^2)^{1/2} \qquad (2)$$

Choosing $D < 0$ for use below, the lower ($\frac{3}{2}$) doublet is primarily composed of the $M_S = \pm\frac{3}{2}$ states, the upper ($\frac{1}{2}$) doublet the $M_S = \pm\frac{1}{2}$ states.

An external magnetic field splits the Kramers doublets and the energies of the resultant states are given by McGarvey (ref 17, eq 111), for the field along $x$, $y$, and $z$ axes. For $g_i\beta H/|\Delta| \ll 1$ only intradoublet transitions are observable and the two Kramers doublets can be viewed as independent EPR-active

**Table II.** Spin-Hamiltonian Parameters[a] for Some $S = 3/2$ Complexes

| Compound | $D$ ($cm^{-1}$) | $\lambda$ | $g$ | $A$ ($cm^{-1} \times 10^4$) | $B$ ($cm^{-1} \times 10^4$) | Ref |
|---|---|---|---|---|---|---|
| Mn(TPP)($O_2$) | $-2.48 \pm 0.07$ | $0.3257 \pm 0.0003$[e] | $1.995 \pm 0.005$ | $-53.1 \pm 0.5$ | $-82.0 \pm 0.5$ ($y$) | This work |
| $Al_2O_3$ host: Mn(IV) | −0.1969 | 0 | 1.9937 | −70.087 | −70.966 | 19, 20 |
| Cr(III) | −0.1921 | 0 | 1.984 | +16.3 | | 24 |
| V(II) | −0.1621 | 0 | 1.991 | −74.045 | −74.809 | 20 |
| $TiO_2$ host: Mn(IV) | 0.406 | 0.32065 | 2.008 ($x$) | | −77.1 ($x$) | 18 |
| | | | 1.9943 ($y$) | −77.5 | −75.0 ($y$) | |
| | | | 1.9927 ($z$) | | | |
| Cr(III)[b] | 0.685 | 0.206 | 1.97 | +15 | | 22 |
| $SnO_2$ host: Mn(IV) | 0.887 | 0.229 | 1.9879 ($x$) | | −72.7 ($x$) | 21 |
| | | | 1.9870 ($y$) | −75.4 | −70.t ($y$) | |
| | | | 1.9907 ($z$) | | | |
| Cr(III)[b] | 0.728 | 0.205 | 1.975 | 15 | | 23 |
| *tràns*-$[Cr(en)_2X_2]$[c] | $-0.4 \rightleftarrows -0.5$ | $0.023 \rightleftarrows 0.217$ | (1.9765) | (16.5) | | 16 |
| | (−0.504) | (0.071) | | | | 25 |
| *trans*-$[Cr(py)_4XY]^+$[d] | $+0.15 \rightleftarrows +0.25$ | ~0 | 1.99 | | | 26 |
| *trans*-$[Cr(NH_3)_4XY]^+$ | $+0.1 \rightleftarrows +0.t$ | ~0 | 1.99 | | | 26 |
| $[Cr(EDTA)]^-$ | +1.069 | 0.19 | 1.982 ($x$,$y$) | | | |
| | | | 1.987 ($z$) | 17 ± 3 | | 27 |

[a] Symbols are defined in the text; in the absence of explicit signs for $A$, $B$, and $D$, absolute values are implied. For nonaxial hyperfine or anisotropic $g$ tensors, individual principal axis values are given. [b] For comparison purposes, coordinate axes have been permuted to make $\lambda < 1/3$. [c] Ranges are for a series of axial ligands; parentheses refer to *trans*-$[Cr(en)_2Cl_2]^+$. [d] Ranges as in *c*; complexes with heavy-atom axial ligands have additional spin–orbit contributions to $D$ and are omitted. [e] This precision depends on the assumption that $g_y = g_z$.

systems, each with effective spin of $S' = 1/2$. In this limit it is possible to obtain effective $g$ values for the two $S' = 1/2$ systems which are functions of $\lambda$ but independent of $D$. Using the equations for the energy of a quartet state in a magnetic field,[17] we find that the two $g$ tensors are rhombic, with principal values

$$\lambda = 0 \quad \begin{matrix} g_z \geq \{ g_z^{1/2} \\ 3g_z \geq \{ g_z^{3/2} \end{matrix} = g_z\left[\frac{2}{(1+3\lambda^2)^{1/2}} \mp 1\right] \Bigg\} \begin{matrix} \geq g_z(\sqrt{3}-1) \\ \geq g_z(\sqrt{3}+1) \end{matrix} \quad \lambda = 1/3$$

$$\lambda = 0 \quad \begin{matrix} 2g_y \leq \{ g_y^{1/2} \\ 0 \leq \{ g_y^{3/2} \end{matrix} = g_y\left[\frac{1+3\lambda}{(1+3\lambda^2)^{1/2}} \pm 1\right] \Bigg\} \begin{matrix} \leq g_y(\sqrt{3}+1) \\ \leq g_y(\sqrt{3}-1) \end{matrix} \quad \lambda = 1/3 \quad (3)$$

$$\lambda = 0 \quad \begin{matrix} 2g_x \geq \{ g_x^{1/2} \\ 0 \leq \{ g_x^{3/2} \end{matrix} = g_x\left[1 \pm \frac{1-3\lambda}{(1+3\lambda^2)^{1/2}}\right] \Bigg\} \begin{matrix} \geq g_x \\ \leq g_x \end{matrix} \quad \lambda = 1/3$$

These equations are able to describe the superposition EPR spectrum of Mn(TPP)($O_2$), and are particularly appropriate for considering the resolved low-field absorptions near $g \sim 5.4$. As $\lambda$ approaches 1/3, $g_z^{3/2}$ decreases and $g_y^{1/2}$ increases; at $\lambda = 1/3$, if $g_z = g_y = g^{MnO_2}$, then the two become equal to $g^{MnO_2}(\sqrt{3}+1) = 2.732 g^{MnO_2} = 5.472$ if $g^{MnO_2} = g_e$. We then tentatively identify $g_z^{3/2} = g_1^{l} = 5.470$ and $g_y^{1/2} = g_1^{u} = 5.424$, and take the small difference, $g_z^{3/2} - g_y^{1/2} = 0.046$, to indicate that $\lambda$ has not quite obtained the limiting values of 1/3 and that the effective symmetry is thus not purely rhombic. The individual $g$ values are used to obtain $g^{MnO_2}$. With $\lambda$ thus available from experiment, $|D|$ may be obtained from the measured energy separation between Kramers doublets, $\Delta$, using eq 2. The assignment of resonance fields and Kramers doublets implies that $D < 0$.

To a small degree, magnitudes of the numbers obtained by this procedure depend on the assumption that $g_z = g_y$. For example, if the complex were in fact purely rhombic, $\lambda = 1/3$, then taking $g_z = 2.0022$ and $g_y = 1.9853$ would reproduce the splitting between $g_1$ resonances which is used to obtain $\lambda = 0.3257$. Indeed, if we take $\lambda = 1/3$, but we interchange assumed $g$ values ($g_z = 1.9853$ and $g_y = 2.0022$), or make an analogous assumption, this would again reproduce the splitting of $g_1$ resonances, but would interchange their assignments to the Kramers doublets, and lead to the result $D > 0$. This is unlikely because of the typically small $g$ anisotropy, with $g_i < 2.0$, of quartet-state ions. Thus in the absence of definite evidence to the contrary, and with the further support of an argument given below, we retain the initial assignment as most probable and accept the conclusion $D < 0$. Further experiments are, however, under way as confirmation.

Proceeding with the assignment $D < 0$, we can identify $A_z = A_z^{3/2} = 57$ G and $A_y = A_y^{1/2} = 88$ G. The extreme $^{55}Mn$ hyperfine anisotropy contrasts markedly with the isotropic coupling of Mn(TPP)(py).

With estimates available for all parameters in the spin-Hamiltonian, resonance positions for the external field along the principal axis directions were then calculated using program EPR, and the parameters refined through systematic comparison with observation. In all but the final variations hyperfine terms were ignored to save computer time, and the centers of the two resolved hyperfine patterns were compared with the appropriate theoretically calculated resonance field; hyperfine tensor components could be calculated from the measured splittings and the correct perturbation theory equations.[18] The values of $|D|$, and thus $|E| = \lambda|D|$, are individually measured to a much lower accuracy than is $\lambda$, since $|D|$ is obtained from the intensity measurements (using $\lambda$ in eq 2); as expected from its large value compared to the microwave quantum, calculated field positions are quite insensitive to $|D|$. Final values for the spin-Hamiltonian parameters are given in Table II, with the negative sign of $D$ retained. The resonance fields calculated from these parameters are in satisfactory agreement with the observed features in the Mn(TPP)($O_2$) EPR spectra; with hyperfine splittings omitted, they are shown in Figure 3.

The only other manganese-containing compounds known to exhibit an $S = 3/2$ ground state involve Mn(IV) ions incor-

porated into a diamagnetic oxide lattice as host. Table II presents the bulk of the available data[18-21] for comparison and indicates the unusual magnetic properties of Mn(TPP)($O_2$). The value of $D$ for the dioxygen complex is almost threefold larger than the largest reported for an oxide lattice, and this difference does not appear to reflect the effects of nitrogen coordination by the porphyrin ligand. We first note that the results quoted for the isoelectronic $d_3$ ions, V(II), Cr(III), and Mn(IV), show that the balancing effects of charge and covalency produce comparable ($TiO_2$,[18,22] $SnO_2$[21,23] hosts) or even largely identical ($Al_2O_3$ host)[19,20,24] values of $D$ for the three ions when placed in the same environment. Next we see that the values of $D$ for Cr(III) ions in an oxide lattice and in a compound possessing four equatorial nitrogen atoms[16,25-27] fall into the same range. As final proof that the porphyrin itself does not produce an anomalously large $D$, we have obtained preliminary results indicating that $D \lesssim 0.2$ cm$^{-1}$ for ClCr$^{III}$(TPP)(py).

In addition, the large $^{55}$Mn hyperfine anisotropy is unique among first- and second-row $S = \frac{3}{2}$ systems.[28] No previously reported Mn(IV) or Cr(III) system shows more than a few percent difference between $A_z$ and $A_y$ for the transition ion nuclear hfs (Table I).[29] Indeed, the great difficulty in obtaining the $^{53}$Cr (9.54% abundant) hfs accurately makes it uncommon to reliably observe *any* deviations from isotropy.

Thus the magnetic properties of Mn(TPP)($O_2$) reflect an $S = \frac{3}{2}$ ground state for the complex, but one with atypical spin-Hamiltonian parameters.

## Discussion

**Analysis of Optical Spectrum.** The similarity between the optical spectra of the reversibly formed Mn(TPP)($O_2$) and an Mn$^{III}$(TPP)(X) (Table I) is striking when it is recalled that such a spectrum, particularly the split Soret peak, is an exception to the metalloporphyrin norm.

The original explanation of the Mn$^{III}$(TPP)(X) spectrum is that of Boucher,[11a] who suggests that the spectrum reflects strong interactions between metal-d and porphyrin-$\pi$ orbitals. Crossing the periodic table from Sc to Zn, the metal d orbitals are stabilized and he proposed that for Mn(III) the ligand–metal interaction is fortuitously at its strongest. The near-ir bands (labeled peaks I, II), one of the two bands (III, IV) between 550 and 650 nm, and the 470-nm peak (V) are all proposed to correspond to ligand-to-metal charge transfer transitions. Recent resonance Raman studies[11b,c] have instead led to the suggestion[11c] that III and IV are the typical 0-0 and 0-1 components of the Q-band, and that V is a mixed charge-transfer, $\pi$–$\pi^*$ transition.

Accepting either analysis for the Mn$^{III}$(TPP)(X) spectra, the similarity of the dioxygen adduct spectrum requires that the manganese d orbitals be at very similar energies in the two instances, and naturally suggests that manganese in the dioxygen adduct be assigned a trivalent formal oxidation state. Assignment of the near-ir bands to charge-transfer transitions further implies that the manganese $d_{xz}$, $d_{yz}$ orbitals cannot be fully occupied in the dioxygen adduct.

**$S = \frac{3}{2}$ ($d^3$) Transition-Ion Interpretation.** Since the Mn(TPP)($O_2$) complex has $S = \frac{3}{2}$ and *no* measurable spin density on $O_2$, it is natural to seek an understanding of the unusual magnetic properties by an analysis in terms of a high-spin $d^3$ ion. In so doing we treat the complex as though it contained three unpaired d electrons on a Mn(IV) ion residing in a strong crystal field provided by the porphyrin and dioxygen ligands; the implications of this treatment are temporarily deferred. In an analysis which closely follows that of McGarvey,[25] we consider that coordination of dioxygen reduces the symmetry at manganese from fourfold to twofold, $C_{2v}$ in our case. The (primed) crystal-field coordinate system is chosen to have $z'$ along the porphyrin normal and to have $x'$ and $y'$ bisect the angles between N atoms. Thus, the "in-plane" pure d orbital pointing between the nitrogens and lying lowest in energy is $d_{x-y^2}$', and the higher-lying in-plane orbital is $d_{xy}$'.

The cardinal feature introduced by the reduction to twofold symmetry is that mixing among d orbitals becomes allowed. If the plane formed by Mn plus $O_2$ does not cut the porphyrin plane along a line between diagonally opposed nitrogens there is mixing between e and $t_2$ orbitals. In particular, for dioxygen lying in $x'z'$ the three-electron determinant of the normal $^4(t_2^3)$ ground-state electron configuration is constructed from the following orbitals: $d_{yz}$'; $d_{xz}$'; and "$x^2 - y^2$" = $ad_{x^2-y'^2} - bd_{z'^2}$, where $a^2 + b^2 = 1$ and the parameter $b^2$ is a measure of the rhombic crystal field component. Accounting for a rhombic distortion by writing the wave function in this way is equivalent in a $d^3$ ion to including configuration interaction (ci) between the ground $^4(t_2^3)$ state and one of the orbital components of a higher $^4T_1$ ($t_2^2e$) state.[25]

**(a) Hyperfine Splittings.** Applying first-order perturbation theory to the hyperfine terms in the original Hamiltonian and employing the $^4(t_2^3)$ determinant built up from the d orbitals given above, we obtain the following formulas for the spin Hamiltonian hyperfine parameters:[30]

$$A_{z'} = P[4(1 - a^2 + b^2)/21 - K]$$
$$A_{x'} = A_{y'} = P[-2(1 - a^2 + b^2)/21 - K] \qquad (4)$$

where, for the free Mn(IV) ion,[31]

$$P = g_e g_{Mn} \beta_e \beta_n \langle r^{-3} \rangle = 235 \times 10^{-4} \text{ cm}^{-1}$$

and where $g_{Mn} = 1.384$ is the $^{55}$Mn nuclear $g$ factor, $\beta_n$ is the nuclear magneton and $\langle r^{-3} \rangle = 5.361$ au is the expectation value of $r^{-3}$ over a free $Mn^{4+}$ ion 3d wave function; $K$ measures the isotropic coupling, $a_i = -PK$. As required, in the absence of orbital mixing ($b^2 = 0$) the half-filled t subshell gives an isotropic hfs.

The measured hyperfine intervals give only the magnitudes of $A_z$ and $A_y$. $P$ is positive for manganese and $a_i$ is generally negative for first row transition ions,[32] and has been shown to be so for a variety of $Mn^{2+}$ ions[32] and also for $Mn^{4+}$ ion (Table II). We thus choose $A_z$ and $A_y$ to be negative, $A_z = -53.1 \times 10^{-4}$ cm$^{-1}$ and $A_y = -82.0 \times 10^{-4}$ cm$^{-1}$. This observed anisotropy can then be described by eq 4 if the principal ZFS axis ($z$) and hyperfine splitting axis ($z'$) are parallel: that is, if $A_z = A_{z'}$ and either $A_y = A_{y'}$ or $A_y = A_{x'}$. We then obtain the values $b^2 = 0.217$, $a_i = -PK = -72.4 \times 10^{-4}$ cm$^{-1}$.

We first note the large value of $b^2$ indicating extensive d-orbital mixing caused by binding of the dioxygen ligand. (This value would be increased if $P$ was taken to be reduced from the free ion value by covalency effects.) Secondly, although the large degree of anisotropy caused by this orbital mixing is unique among $S = \frac{3}{2}$ ions, as may be seen by the representative hyperfine splittings in Table II, nevertheless $a_i$ is quite comparable to that for Mn(TPP)(py) and for the Mn(IV) ions which have been studied. This result in turn supports the assignment $A_z = A_{z'}$ and therefore the conclusion that $D <$ 0.

**(b) Zero-Field Splittings.** In the crystal-field model with a ci $^4(t_2^3)$ ground state, the zero-field splitting is caused by spin-orbit interaction with $^4(t_2e)$, $^2(t_2^2e)$, and $^2(t_2^3)$, and with charge-transfer excited states and by direct spin–spin interaction. The latter interaction may be estimated using the expansion of Pitzer, Kern, and Lipscomb[33] and evaluating the radial integrals with Slater orbitals. We find a spin–spin contribution of $D_{ss} \sim +1.5b^2$ cm$^{-1}$ $\sim +0.33$ cm$^{-1}$ (principal axis along $z'$), roughly 10% of the magnitude of the observed value.

If the ci ground state already contains a substantial excited state conribution ($b^2 \neq 0$) then spin–orbit contributions to

*both D* and *E* become large. However, even though $b^2$ may be obtained directly from the analysis of hyperfine splittings, use of McGarvey's[25] equations to calculate *D* and *E* for Mn(TPP)($O_2$) would require observation of the d–d absorption bands, and this is precluded by the intensity of the porphyrin optical transitions. Moreover, the numerous low-lying charge-transfer excited states expected to occur in Mn(TPP)($O_2$) (vide infra) may be expected to contribute to an extent not found in "simple" Cr(III) complexes. Thus, it seems that only detailed MO calculations in this system, such as some presently under way,[34] can be used to analyze in detail the excited-state contributions to *D* and *E*. These calculations will further examine the actual significance of the large orbital mixing indicated through use of the first-order hyperfine expressions, eq 4.

However, there is one feature of McGarvey's treatment which must be noted. He finds that the rhombic interaction which gives rise to a nonzero $b^2$ also produces a major reorientation of the principal axes of the zero-field splitting, causing it to be normal to the *z'* axis. Indeed, as an instructive example, we have employed the optical parameters appropriate to *trans*-$[Cr(en)_2Cl_2]^+$[25] and the directly measured value $b^2 = 0.217$ to estimate a theoretical *D* and *E* for Mn(TPP)($O_2$). Although of primarily illustrative value, the procedure is not wholly unreasonable; we recall that *D* is largely charge independent, as shown by comparing isoelectronic $d^3$ ions in a given host (Table II). The calculations turn out to be sensitive primarily to the value of $b^2$. The calculated *D* and *E* are of comparable magnitude to those observed, and the *z* axis of the ZFS tensor is in fact calculated to be normal to *z'*.

Thus, in addition to an examination of the theoretical predictions,[34] measurements in an oriented (single-crystal) or partially oriented (liquid crystal) system[35,36] would clearly be important in order to determine whether the principal axis of the ZFS lies along the normal to, or in the plane of, the porphyrin.

**Spin Coupling Models.** The EPR spectrum of Mn(TPP)($O_2$) has been successfully analyzed as resulting from a quartet state molecule, and this success rules out certain formulations for the electronic structure of the adduct: (i) (high-spin Mn(II))($^1O_2$); (ii) (low-spin Mn(III))($O_2^-$). However, the resulting spin Hamiltonian parameters have been interpreted in terms of an $S = 3/2$, $d^3$ ion, whereas certain "spin-coupling" schemes may be envisaged which also give rise to a spin-quartet complex; (iii) spin-coupled (high spin Mn(II))-($^3O_2$); and (iv) spin-coupled (high spin Mn(II))($O_2^-$). One concrete form "spin-coupling" could take is mathematically expressed by the addition of an isotropic exchange term to the zeroth order Hamiltonian describing noninteracting metalloporphyrin and dioxygen moieties in the particular valency and spin-states chosen. In Appendix A we examine such a form of models iii and iv, and show that they are unable to explain the absence of $^{17}O$ hfs in Mn(TPP)($O_2$) and thus may be eliminated from consideration.

**Electronic Structure.** The optical spectrum for Mn(TPP)($O_2$) resembles those of $Mn^{III}$(TPP)(X) (Table I), suggesting considerable Mn → $O_2$ charge transfer upon adduct formation, and a bonding formulation in terms of covalent interactions between $Mn^{III}$(TPP) and a superoxo fragment. On the other hand, the observation of a quartet ground state for Mn(TPP)($O_2$), the successful interpretation of the hfs anisotropy in terms of a $^4(t_2^3)$ transition ion, in this case therefore an $Mn^{IV}$ ion, and the absence of spin-density on dioxygen naturally suggest as the formal valence state of the complex, $Mn^{IV}(O_2^{2-})$.

The contradiction between the two formal views is, of course, in a sense more apparent than real. It is clear that the similar electronic transition energies for the oxidized and oxygenated porphyrins require that the $t_2$ orbital energies of the two systems be similar, and thus the overall charges on manganese are probably similar also. However, the observation of ligand–metal charge-transfer transitions merely requires that the $d_{xz}$, $d_{yz}$ orbitals not be completely filled, and this is consistent with either high-spin $d^3$ or $d^4$ ions. Moreover, it is also clear that the principle of electroneutrality would rule out the actual existence of an "$Mn^{4+}$" ion. Indeed, in one comparison of the isoelectronic ions, "$V^{2+}$", "$Cr^{3+}$", and "$Mn^{4+}$", it was suggested that charge transfer occurs in each case to the extent that the actual metal–ion charge is +2 or less.[25]

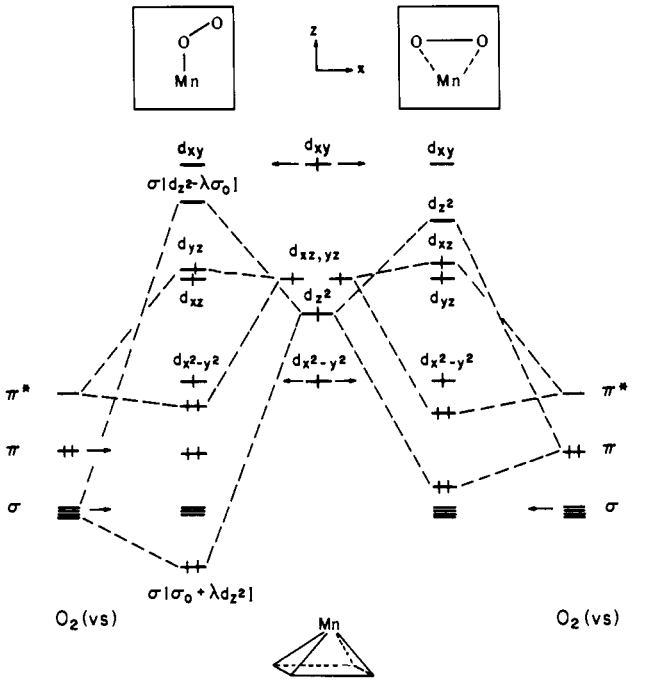


**Figure 5.** Schematic MO diagram for $O_2$ binding to Mn(TPP). For discussion, see text. Note that for convenience primes have been left off the axis designations.

Nevertheless, examinations of the bonding in this unusual complex in terms of a simple qualitative energy-level scheme allow us to rationalize the unusual intermediate ($S = 3/2$) spin-state in terms of a $^4(t_2^3)$ ion configuration, to confirm the intuitive notions of an extensive degree of metal "oxidation", and to assign a formal valency to the metalloporphyrin and dioxygen fragments of the adduct.

We approach the bonding in Mn(TPP)($O_2$) by construction of an interaction diagram between Mn(TPP) and dioxygen fragments. Since the absence of an additional coordinating base suggests that the manganese atom lies out-of-plane toward $O_2$, the basis orbitals for Mn(TPP) (Figure 5) are taken to be those of a pyramidal $ML_4$ fragment as presented by Hoffmann and co-workers.[37] We assume the plane of the metal and oxygen atoms to be the *x'–z'* plane, and shall make use of reflection with respect to *xz'* to classify the basis orbitals.

The dioxygen fragment is presented, following Griffith,[38] in its valence state (vs). This state has molecular orbitals very similar to those of ethylene and indeed may be (conceptually) constructed by taking ethylene and merging the protons with the nucleus of the carbon atom to which they are respectively bonded. There are four $sp^2$ lone-pairs lying in a plane with the oxygen nuclei, and a doubly-occupied $\pi$ bonding orbital and an empty $\pi^*$ antibonding orbital normal to the plane. This hybridization of $O_2$ is especially convenient for considering coordination by a single O atom, with a bent geometry (vide infra), and for comparing this mode of bonding with the edge-on, "ethylene-like" structure. We shall not discuss a linear model because the resulting $C_{4v}$ geometry would require $E = 0$, by symmetry.

Although the energy spacings in Figure 5 are basically schematic, the ordering deserves comment. The disposition of the energy levels of pyramidal Mn(TPP) is discussed by Hoffmann et al. in their considerations of bonding to NO.[37] However, the oxygen orbitals enter the interaction picture below the metal d orbitals, unlike the situation for NO; the $O_2$ orbitals must be placed much lower than those of NO in order to reflect the ~3 eV greater ionization potential of $O_2$.[39] The d orbitals of MnTPP will also be higher than those of Co(TPP) further indicating that the ordering will differ from that presented for bonding in Co-$O_2$ complexes.[37b] Note, however, that the absence of spin density on dioxygen requires that all three unpaired electrons be in orbitals which are predominantly of d character, and that none be in orbitals of predominantly dioxygen $\pi$-character. This makes the following discussion insensitive to the particular details of Figure 5.

In the symmetric, edge-on geometry

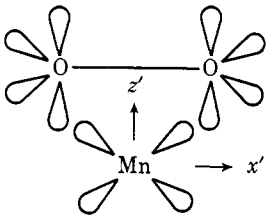


the $\pi$ and $\pi^*$ orbitals on $O_2$ (vs) lie in the triatomic plane. Two bonding interactions occur, as shown schematically in Figure 5. There is $\sigma$ mixing between $d_{z'}$ and $\pi$ (vs), and $\pi$ interaction between the metal $d_{xz'}$ and $\pi^*$ (vs). Specifying the orbital occupations leaves three electrons in levels which are not only primarily of metal d character, but which also correspond to the $^4(t_2^3)$ configuration to be expected as the ground state of a $d^3$ ion in a tetragonally-distorted environment (Figure 5). Thus, the bonding scheme is consistent with the observed EPR results and their natural interpretation in terms of a Mn(IV), $d^3$ ion.

Furthermore, as noted above, the assignment of various of the optical bands to ligand → metal charge transfer transitions requires merely that the $d_{xz'}$, $d_{yz'}$ levels be half-filled, and this is true in our present scheme. If the two near-ir bands in $Mn^{III}$(TPP)(py) correspond separately to charge transfer into $xz'$ and $yz'$, then the observation of but a single band in Mn(TPP)($O_2$) may reflect the raising of $d_{xz'}$ through its interaction with $\pi^*$ and thus a shift of that transition to higher energy.

The principal change in electron distribution is seen to be the pairing of two electrons from the MnTPP fragment, one from $d_{z^2}$, and the other, $d_{xy'}$, and their transfer to the bonding $\pi^*$, $d_{xz'}$ combination. Since $\pi^*$ (vs) is substantially lower than $d_{xz'}$, the bonding orbital will be predominantly $\pi^*$, and thus we see that adduct formation in fact corresponds to extensive M → $O_2$ charge transfer. Because two "metal electrons" become largely dioxygen in character upon adduct formation, it is also clear that the *formal* $Mn^{IV}(O_2^{2-})$ valency formalism is to be preferred.

This picture can also accommodate the absence of observed $^{17}O$ hyperfine splittings. First, the $\sigma$ bond between $d_{z^2}$ and $\pi$ is certainly the strongest metal-dioxygen interaction. Since the resultant combination orbitals are either empty or doubly occupied, no odd-electron density is involved. Second, if the $\pi^*$-$d_{xz'}$ mixing is, as expected, small, then the half-filled antibonding combination will be almost completely metal $d_{xz'}$ in character and minimal spin transfer to $\pi^*$ would occur. Although it might appear unusual to place an odd electron in an orbital which can by symmetry have $\pi^*$ character, but yet not observe $^{17}O$ hfs, we recall that superhyperfine splittings are typically difficult to observe in $d^3$ ions,[17] and that an even more striking situation must occur in the binding of pyridine or imidazole to $Mn^{II}$TPP. In this latter case we have the strong interaction between a filled ligand long-pair and a half-filled $d_{z^2}$ orbital, yet no $^{14}N$ hfs from the nitrogenous base is observed.

We note in passing that it is possible to imagine a stronger degree of $\pi$ interaction, raising $d_{xz'}$ in energy to the point that other odd-electron configurations, corresponding to $^4(t_2^2e)$, would result. Such strong $\pi$-bonding seems implausible in principle and further appears unlikely in the face of the relatively low affinity of MnTPP for $O_2$ vs. pyridine. Furthermore, the observed hyperfine splittings anisotropy also makes such configurations unattractive.[40]

Considering a "bent" coordination geometry, the valence state hybridization of $O_2$ naturally suggests an 120° angle

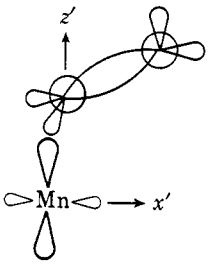


with one of the four lone-pairs lying along $z'$ and with $\pi$ and $\pi^*$ normal to the triatomic plane. As in the symmetric geometry, again two bonding interactions occur (Figure 5). There is $\sigma$-mixing between $d_{z^2}$ and $\sigma$ (vs) and a $\pi$-interaction between $\pi^*$ (vs) and $d_{yz'}$.

We can be brief in discussing this situation, because it offers no new features over that presented above. Again, we see the $^4(t_2^3)$ electron configuration and the substantial M → $O_2$ charge transfer, with a transfer of two d electrons to a primarily $O_2$ (vs) orbital. Thus, both geometries should be considered to correspond to the $Mn^{IV}(O_2^{2-})$ formalism, with the presence of a ground-state $d^3$ ion. In addition, the considerations about $^{17}O$ hfs can be repeated without appreciable change.

**Geometry.** Among the three plausible limiting Mn-$O_2$

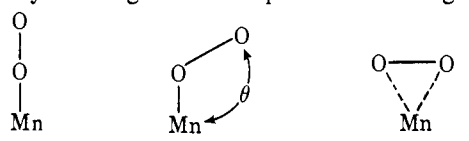


geometries we eliminate I from consideration on the basis of the EPR results. The resulting $C_{4v}$ complex could not, by symmetry, exhibit the large $\lambda$ which we observe. Geometries II and III have the required reduced symmetry and have been shown to give rise to quite similar bonding patterns: each exhibits one $\sigma$ and one $\pi$ bonding interaction. Because the formal $Mn^{IV}(O_2^{2-})$ valency applies, analogy with other peroxo complexes[41] suggests geometry III is to be favored. Although it might be anticipated that steric hindrance between dioxygen and the nitrogens of TPP would disfavor III, it has recently been shown that Ti(octaethylporphyrin)($O_2$) in fact adopts geometry III.[42] Thus, we reiterate our tentative suggestion[7] that the symmetric mode of bonding (III) obtains in this adduct.

However, the situation is not simple. The principal difference between gometries II and III would appear to be in steric factors and in the nature of the $\sigma$ bond which is formed. Both geometries can be viewed as exhibiting the strong $\sigma$-donation of an electron-pair from the dioxygen moiety, but with different donor orbitals being utilized: the geometry preferred must then largely be determined by the relative donating abilities of the filled $\pi$ (geometry III) and the $\sigma$ (geometry II) dioxygen orbitals. Although the former will be closer in energy to $d_{z^2}$, favoring III, a more effective overlap between $d_{z^2}$ and $\sigma$ (vs) should favor II. We need merely note that analogous consid-

erations of $\sigma$-donor abilities suggested that $\pi \rightarrow d_{z^2}$ is more favorable than $\sigma \rightarrow d_{z^2}$, and thus gave rise to the erroneous prediction that an Fe-$O_2$ linkage would adopt III.[38,43] A variety of experiments can be imagined which can in principle interrogate the molecule as to the equivalence of the two O atoms and some of these are underway.

## Conclusions

Both optical and EPR measurements have shown the reversible coordination of dioxygen to $Mn^{II}TPP$. The adduct formed is seen to be Mn(TPP)($O_2$), without an additional coordinating base, and the equilibrium constant for replacing a metal-bound pyridine by $O_2$ is less than unity (−79 °C).

The EPR results indicate a quartet state molecule, and qualitative bonding considerations support (i) the notion of substantial $Mn \rightarrow O_2$ charge transfer, and (ii) the utility and propriety of an $Mn^{IV}(O_2^{2-})$ valency formalism[44] in which the Mn(IV) is in the $^4(t_2^3)$ ground state. A linear geometry can be ruled out on the basis of the EPR observations, and, although definite conclusions about structure are not possible at this time, we tentatively favor the symmetric, "edge-on" structure.

Now that it has been shown that Mn(TPP) is an oxygen carrier at low temperatures, other approaches which prevent irreversible oxidation might successfully stabilize the dioxygen adduct at higher temperatures. For the iron(II) systems, these included the utilization of steric factors and also attachment of the iron(II) complex to a rigid surface.[2] The latter approach has in fact recently been shown to work for the system silica gel-Mn(TPP).[45] This third observation of reversible dioxygen binding by a first-row transition metal, as well as the apparently irreversible binding of an $O_2$ moiety to a titanium porphyrin,[42] clearly suggests that complexes of other metals such as chromium(II)[46] and vanadium(II) should be similarly examined.

**Acknowledgment.** This research was supported by grants from the National Institutes of Health, National Science Foundation, and the donors of the Petroleum Research Fund, administered by the American Chemical Society. B.M.H. is the recipient of a National Institutes of Health Career Development Award.

## Appendix. Spin Coupling Models

**(a) (High-Spin $Mn^{II}$)($^3O_2^-$).** By the rules for coupling angular momenta, an ($S = 5/2$) $Mn^{II}$(TPP) can spin-couple with an $S = 1$ dioxygen to form joint states with total spin $S_T = 7/2, 5/2, 3/2$. This coupling is described by augmenting the spin-Hamiltonian for high-spin $Mn^{II}$(TPP), plus that for $^3O_2$, with a spin-coupling term $H_c = JS^{Mn} \cdot S^O$. Observation of a ground state quartet is in this picture indicative that $J$ is large and positive.

Through straightforward application of the Wigner-Eckart theorem[31] it is possible to relate the spin-Hamiltonian parameters for the $S = 3/2$ complex to those of the isolated components. The $^{17}O$ nuclear hyperfine constant is of particular utility as a test for the model, and we find that a coupling constant $A_i^{^3O_2}(^{17}O)$ for a $O_2(^3\Sigma)$ molecule would give rise to a coupling constant in Mn(TPP)($O_2$) of $A_i^{MnO_2}(^{17}O) = -(2/5)A_i^{^3O_2}$. Since the $^{17}O$ hyperfine coupling on $O_2(^3\Sigma)$ is large, this model would require a substantial hyperfine coupling in the $^{17}O$ enriched dioxygen adduct, and is contradicted by our experiments.

**(b) Spin-Coupled (high spin $Mn^{III}$)($O_2^-$).** If an ($S = 2$) $Mn^{III}$(TPP) is spin coupled to an $S = 1/2$ superoxide ion (with quenched orbital angular momentum) by a term $H_c$ with $J$ large and positive, then a ground quartet again results. This model yields $A_i^{MnO_2}(^{17}O) = -(1/5)A_i^{O_2^-}$. Although a substantial reduction in coupling constant is predicted, $^{17}O$ has a nuclear spin of $I = 5/2$, and the overall spread of the hyperfine pattern would be $5A_i^{MnO_2}(^{17}O) = -A_i^{O_2^-}$. Since $A_z^{O_2^-} \sim 60$–$90$ G,[47,48] such a pattern could not go undetected in our spectra, and thus this model too is contradicted by experiment.

## References and Notes


(1) Authors to whom correspondence should be addressed.
(2) F. Basolo, B. M. Hoffman, and J. A. Ibers, *Acc. Chem. Res.*, **8**, 384 (1975), and references therein.
(3) B. M. Hoffman, Q. H. Gibson, C. Bull, R. H. Crepeau, S. J. Edelstein, R. G. Fisher, and M. J. McDonald, *Ann. N.Y. Acad. Sci.*, **244**, 174 (1975).
(4) D. L. Anderson, C. J. Weschler, and F. Basolo, *J. Am. Chem. Soc.*, **96**, 5599 (1974); G. C. Wagner and R. J. Kassner, *ibid.*, **96**, 5593 (1974); W. S. Brinigar and C. K. Chang, *ibid.*, **96**, 5595 (1974); J. Almag, J. E. Baldwin, R. L. Dyer, J. Huff, and C. J. Wilkerson, *ibid.*, **96**, 5600 (1974).
(5) J. A. Elvidge and A. B. P. Lever, *Proc. Chem. Soc., London*, 195 (1959); L. H. Vogt, Jr., A. Zalkin, and D. H. Templeton, *Inorg. Chem.*, **6**, 1725 (1967).
(6) J. H. Fuhrhop, K. M. Kadish, and D. G. Davis, *J. Am. Chem. Soc.*, **95**, 5140 (1973).
(7) C. J. Weschler, B. M. Hoffman, and F. Basolo, J. Am. Chem. Soc., **97**, 5278 (1975).
(8) B. Gonzalez, J. Kouba, S. Yee, C. A. Reed, J. Kirner, and W. R. Scheidt, *J. Am. Chem. Soc.*, **97**, 3247 (1975).
(9) H. Kobayashi and Y. Yanagawa, *Bull. Chem. Soc. Jpn.*, **45**, 450 (1972).
(10) M. J. Carter, D. P. Rillema, and F. Basolo, *J. Am. Chem. Soc.*, **96**, 392 (1974).
(11) (a) L. J. Boucher, *Coord. Chem. Rev.*, **7**, 289 (1972); *J. Am. Chem. Soc.*, **92**, 2725 (1970); (b) R. R. Gaughan, D. F. Shriver, and L. J. Boucher, *Proc. Natl. Acad. Sci. U.S.A.*, **72**, 433 (1975); (c) J. A. Shelnutt, D. C. O'Shea, N.-T. Yu, L. D. Cheung, and R. H. Felton, *J. Chem. Phys.*, **64**, 1156 (1976).
(12) C. J. Weschler, D. L. Anderson, and F. Basolo, *J. Am. Chem. Soc.*, **97**, 6707 (1975).
(13) (a) B. M. Hoffman and D. Mahoney, unpublished; (b) B. M. Hoffman and C. A. Reed, unpublished.
(14) T. Yonetani, H. Yamamoto, J. E. Erman, J. S. Leigh, Jr., and G. H. Reed, *J. Biol. Chem.*, **247**, 2447 (1972).
(15) W. E. Blumberg, unpublished.
(16) J. E. Hempel, L. O. Morgan, and W. B. Lewis, *Inorg. Chem.*, **9**, 2064 (1970).
(17) B. R. McGarvey, *Transition Met. Chem.*, **3**, 89 (1967).
(18) H. G. Andresen, *Phys. Rev.*, **120**, 1606 (1960); *J. Chem. Phys.*, **35**, 1090 (1961).
(19) S. Geschwind et al., *Phys. Rev.*, **126**, 1684 (1962).
(20) N. Laurance and J. Lambe, *Phys. Rev.*, **132**, 1029 (1963).
(21) W. H. From, P. B. Dorain, and C. Kikuchi, *Phys. Rev. A*, **135**, 710 (1964).
(22) H. J. Gerritsen et al., *Phys. Rev. Lett.*, **2**, 153 (1959).
(23) W. H. From, *Phys. Rev.*, **131**, 961 (1963).
(24) R. W. Terhune, J. Lambe, C. Kikuchi, and J. Baker, *Phys. Rev.*, **123**, 1265 (1961).
(25) B. R. McGarvey, *J. Chem. Phys.*, 41, 3743 (1964).
(26) E. Pedersen and H. Toftlund, *Inorg. Chem.*, **13**, 1603 (1974).
(27) R. Aasa, K. E. Falk, and S. A. Reyes, *Ark. Kemi*, **25**, 309 (1966).
(28) Re(IV) is highly anisotropic in $SnO_2$: H. H. Piper and K. Schwochau, *J. Chem. Phys.*, **63**, 4716 (1975).
(29) The reported anisotropies in bisoxalatochromium (III) complexes (H. Andriessen, *Inorg. Chem.*, 14, 792 (1975)) are not in fact significant.
(30) Formulas given in ref 29 are incorrect.
(31) A. Abragam and B. Bleaney, "EPR of Transition Ions", Oxford University Press, London, 1970.
(32) B. R. McGarvey, *J. Phys. Chem.*, **71**, 51 (1967).
(33) R. M. Pitzer, C. W. Kern, and W. N. Lipscomb, *J. Chem. Phys.*, **38**, 1607 (1963).
(34) M. R. Ratner, B. M. Hoffman, and F. Basolo, unpublished.
(35) J. P. Fackler, J. D. Levy, and J. A. Smith, *J. Am. Chem. Soc.*, **94**, 2436 (1972), and references therein.
(36) B. M. Hoffman, F. Basolo, and D. L. Diemente, *J. Am. Chem. Soc.*, **95**, 4697 (1973).
(37) (a) R. Hoffmann, M. M. L. Chen, M. Elian, A. R. Rossi, and D. M. P. Mingos, *Inorg. Chem.*, **13**, 2666 (1974); see also (b) B. B. Wayland, J. V. Minkiewicz, and M. E. Abd-Elmageed, *J. Am. Chem. Soc.*, **96**, 2795 (1974).
(38) J. S. Griffith, *Proc. R. Soc. London, Part A*, **235**, 23 (1956).
(39) "CRC Handbook of Chemistry and Physics", 54th ed, C. R. Weast, Ed., Chemical Rubber Co., Cleveland, Ohio, 1973.
(40) The equations for the ($t_2^2e$) configuration with electrons in "$x^2 - y^2$", $yz'$, and "$z^{2'}$" = $ad_{z^2} + bd_{x^2-y^2}$ are independent of $b$ and thus of orbital mixing: $A_{x'} = P[-4/7 - K]$; $A_{y'} = A_{z'} = P[-2/7 - K]$. Assigning $A_z = A_{x'}$, then the observed anisotropy is describable in principle. However, we obtain the unlikely[31] value $a_i = +8 \times 10^{-4}$ cm$^{-1}$. For the $^4(t_2^2e)$ configuration with electrons in "$x^2 - y^2$", $yz'$, and $xy'$, we obtain $A_{x'} = P[-4b^2/21 - K]$; $A_{y'} = P[2(3 - 2b^2)/21 - K]$; $A_{z'} = P[-2(3 - 4b^2)/21 - K]$. These equations may be used if $A_z = A_{x'}$ and $A_y = A_{y'}$. If $P$ is taken to be ~80% of the free ion value, then $b^2 \sim 0.2$, but the calculated $a_i = -46 \times 10^{-4}$ cm$^{-1}$ is still of unusually low magnitude. However, we note that s–d mixing is symmetry allowed and would give positive contributions to $a_i$.
(41) See J. S. Valentine, *Chem. Rev.*, **73**, 235 (1973).
(42) R. Guilard, M. Fontesse, and P. Fournari, *J. Chem. Soc., Chem. Commun.*, 161 (1976).
(43) D. M. P. Mingos, *Nature (London), Phys. Sci.*, **230**, 154 (1971).

(44) For those who relish theological disputation and wish to quarrel with our adoption of a formal valency, we refer to the quite recent review, L. Vasko, *Acc. Chem. Res.*, **9**, 175 (1976).
(45) O. Leal and C. J. Weschler, private communication.
(46) It has recently been found that solid $Cr^{II}(TPP)(py)$ irreversibly binds dioxygen, C. A. Reed, private communication.
(47) E. F. Vansant and J. H. Lunsford, *Adv. Chem. Ser.*, **No. 121**, 441 (1973).
(48) E. Melamud, B. C. Silver, and Z. Dori, *J. Am. Chem. Soc.*, **96**, 4689 (1974).

# Protein Control of Porphyrin Conformation. Comparison of Resonance Raman Spectra of Heme Proteins with Mesoporphyrin IX Analogues[1]

**Thomas G. Spiro* and J. Michael Burke**

*Contribution from Department of Chemistry, Princeton University, Princeton, New Jersey 08540.* *Received January 2, 1976*

**Abstract:** Resonance Raman spectra are reported for derivatives of iron mesoporphyrin IX, chosen as analogues for the heme group in heme proteins. Attention is focused on high-frequency porphyrin ring modes which are sensitive to the conformation and electronic structure of the heme group. No protein influence on heme conformation is detectable for low-spin Fe(III) or Fe(II) derivatives nor for high-spin Fe(II) derivatives. For high-spin Fe(III) derivatives, a protein influence is detectable in hemoglobin and myoglobin. The porphyrin frequencies suggest a prophyrin conformation more characteristic of Fe(II) than Fe(III). The heme pocket apparently stabilizes the porphyrin conformation appropriate for high-spin Fe(II) and maintains it on oxidation, thereby contributing to the relatively low oxidation potential of deoxyhemoglobin or myoglobin. Axial ligands of increasing $\pi$ acid strength bound to Fe(II) hemes progressively increase the frequency of the "oxidation state" marker bands. This behavior supports the view that these frequencies are sensitive to the extent of back donation into porphyrin $\pi^*$ orbitals of iron $\pi$ electrons, for which the $\pi$-acid ligands compete. A derivative thought to contain four-coordinate Fe(II) gives frequencies similar to low-spin Fe(III), consistent with an intermediate spin configuration, with empty $d_{x^2-y^2}$ and half-filled $d_{z^2}$, $d_{xz}$, and $d_{yz}$ orbitals. The Raman spectrum of the $(py)_2Fe^{II}$ complex shows vibrational bands of the bound pyridine, enhanced via resonance with a charge-transfer transition at ~475 nm.

The relationship between porphyrin stereochemistry and the biochemical functions of heme proteins continues to be the focus of wide-ranging chemical and physical studies. Previous reports from this laboratory have catalogued the resonance Raman spectra of a number of heme proteins.[2] Observed shifts in porphyrin ring vibrational frequencies have been interpreted[3] in terms of known principles of heme stereochemistry and electronic structure, derived from structural analysis of heme proteins and of metalloporphyrins. In the present study we have examined the resonance Raman spectra of various derivatives of iron mesoporphyrin IX dimethyl ester (abbreviated "MP"), chosen to resemble the prosthetic group of heme proteins in different ligation and oxidation states. The results show that most heme protein resonance Raman spectra are essentially the same as those of the appropriate iron (MP) derivative. In these cases, which include all low-spin hemes as well as five-coordinate high-spin Fe(II) heme, the proteins appear to have negligible influence on the porphyrin conformation. High-spin $Fe^{II}(MP)$ derivatives show spectra appreciably different from those of high-spin Fe(III) hemoglobin or myoglobin derivatives, but they correspond to the spectrum of native horseradish peroxidase, which had previously been thought to be anomalous.[4] The anomaly resides instead in hemoglobin and myoglobin, which apparently constrain the porphyrin to a more highly domed structure. This globin influence on porphyrin conformation may be a factor in stabilizing high-spin Fe(II) heme, which is a requirement for reversible oxygenation.

## Experimental Section

Mesoporphyrin IX dimethyl ester was purchased from Sigma Chemical Co. and used without further purification. Dimethylformamide was distilled and stored over molecular sieves. Pyridine (py) was distilled and stored over KOH. Imidazole (Im) and 2-methylimidazole (2-MeIm) were recrystallized from benzene. Other ligands were used as purchased. Carbon tetrachloride, chloroform, and dichloromethane were spectroquality solvents and were used without further purification. $D_2SO_4$ (99% D) and $D_2O$ were purchased from Stohler Isotope Chemicals and used without further purification.

**Mesoporphyrin-*meso*-$d_4$ IX Dimethyl Ester (MP-$d_4$).** Mesoporphyrin-*meso*-$d_4$ IX dimethyl ester was prepared by allowing MP to equilibrate in 90% $D_2SO_4/D_2O$ for 12 h.[5] After dilution with $H_2O$ and raising the pH to the isoelectric point with 2 N ammonium hydroxide, the meso deuterated porphyrin was extracted into chloroform. The chloroform layer was washed several times with water to remove acid and allowed to evaporate. Any hydrolyzed porphyrin was re-esterified in $H_2SO_4$/methanol.[6a] The final product was purified by chromatography on Alumina (Fisher A-540) and recrystallized from chloroform. The visible spectrum agreed with MP and the NMR spectrum showed complete disappearance of the meso protons.[7]

**Iron(III) Derivatives.** $(X^-)Fe^{III}(MP)$ [X = F, Cl] and their meso-$d_4$ derivatives were prepared both according to the method of Falk[6b] and the method of Adler et al.[8] Both methods gave similar products as evidenced by their visible[9] and infrared spectra.[9] The final products were purified by chromatography according to the method of Alben et al.[9] and converted to the appropriate halide by heating with the sodium halide in acetic acid. $(Im)_2Fe^{III}(MP)^+$ fluoride and chloride salts, and their meso-$d_4$ derivatives were prepared according to the methods of Epstein et al.[10] The $\mu$-oxo-bis[$Fe^{III}(MP)$] complex was prepared by shaking a $CH_2Cl_2$ solution of an iron(III) halide complex with an aqueous solution of 0.01 N sodium hydroxide.

**Iron(II) Derivatives.** All of the iron(II) derivatives were prepared in a modified Spex spinning cell sealed with a septum. A degassed $CH_2Cl_2$ solution of an $Fe^{III}(MP)$ halide was overlayered with water containing a small amount of $Na_2S_2O_4$ and an excess of the appropriate ligand. All operations were done in an argon atmosphere. The cell was sealed and shaken vigorously until the $CH_2Cl_2$ layer turned from brown to red. The CO derivatives were prepared by bubbling CO through the $Fe^{II}(MP)$ solution.

All spectra were recorded on instrumentation reported previously.[11] Concentration of solutions was about 1 mg/ml.